Available online at www.sciencedirect.com
SCIENCE DIRECT
Journal of Volcanology and Geothermal Research 155 (2006) 138–149
Journal of volcanology and geothermal research
www.elsevier.com/locate/jvolgeores

Proximal tephra hazards: Recent eruption studies applied to volcanic risk in the Auckland volcanic field, New Zealand

B.F. Houghton [a,*], C. Bonadonna [a], C.E. Gregg [a], D.M. Johnston [b], W.J. Cousins [b], J.W. Cole [c], P. Del Carlo [d]

[a] *Geology & Geophysics, University of Hawai'i, 1680 East-West Road, Honolulu, Hawai'i 96822, USA*
[b] *Institute of Geological & Nuclear Sciences, P.O. Box 30368, Lower Hutt, New Zealand*
[c] *Geological Sciences, University of Canterbury, Private Bag 4800, Christchurch, New Zealand*
[d] *Istituto Nazionale di Geofisica e Vulcanologia, Piazza Roma 2, Catania, 95123 Italy*

Received 21 March 2005; accepted 6 February 2006
Available online 20 March 2006

Abstract

Auckland, New Zealand is unique in being a metropolitan area built on an active volcanic field. Despite the small size and intensity of Auckland eruptions, the risk from tephra fall is high because of the high density of buildings and lifelines. The nature of this threat can be evaluated by comparisons with historical Strombolian and Hawaiian eruptions, which have occurred in non-populated areas. Cone-building phases of such eruptions are typically protracted, i.e., weeks to months in duration, prolonging the period during which emergency managers will have to fine tune mitigation for numerous parameters such as fluctuations in intensity and wind shifts. Rapid cone growth during future eruptions will define a region of some 30 to 100 ha where complete destruction will occur on a time scale of hours. The cost of this destruction is likely to range between NZ$200M and NZ$1.4B (ca. US$130M to US$900M). Beyond this, we have modeled the cumulative long-term effect of the build-up of a downwind blanket of lapilli and ash by estimating accumulation rates for three phases of the 1959 Kīlauea Iki eruption in Hawai'i. The effect of changing wind direction was evaluated using low-level wind data from Auckland. These results show that intervals between 4 and 100 h will lapse before onset of significant damage to buildings.

Keywords: tephra hazard; Auckland volcanic field; cone growth; tephra fall

1. Introduction

Most impact assessments for natural hazards assume a short duration for the event such that the studies model the impact of say a flood, earthquake or tsunami in its entirety. An important exception is the evaluation of the progressive cumulative effects of future tephra fall at Soufriere Hills, Montserrat (Bonadonna et al., 2002a,b). The generalization is valid for many volcanic eruptions, particularly those of high eruption intensity where the total duration of explosive activity is short, e.g., 60 h for Novarupta 1912 (Hildreth, 1987), or the climactic 1991 eruption of Pinatubo (Wolfe and Hoblitt, 1996). However, eruptions of low intensity (discharge rate) and cone-building style are often protracted (Richter and Eaton, 1960; Richter et al., 1970; Parfitt and Wilson, 1994; Heliker et al., 1998; INGV Staff, 2001; Acocella and Neri, 2003; Behncke and Neri, 2003; Heliker and

* Corresponding author. Tel.: +1 808 956 2561; fax: +1 808 956 5512.
E-mail address: bhought@soest.hawaii.edu (B.F. Houghton).

0377-0273/$ - see front matter © 2006 Elsevier B.V. All rights reserved.
doi:10.1016/j.jvolgeores.2006.02.006

Mattox, 2003; Calvari and Pinkerton, 2004). Table 1 lists the duration of cone-forming phases of the four best-documented eruptions of this type.

Management of crises of this type requires emergency managers to make mitigation choices *during* the explosive activity that have significant consequences for the levels of discomfort and damage suffered by the community (Barberi et al., 2003). They must also 'fine tune' their response plans innumerable times to take account for variations like waxing and waning of the intensity of the eruption, changing wind velocities and shifts in vent position. All these and other variables may change with very little warning, greatly adding to the stress levels in the decision-making environment. On a more positive note, during such events, Civil Defense has an opportunity to take measures that may greatly reduce the hazardous consequences of the eruption, e.g., damage to buildings, loss of electrical supply, damage to waste water treatment facilities (Barberi et al., 2003).

Table 1
Summary of characteristics of the four eruptions at Kīlauea and Etna [a]

Eruption summary	Kīlauea Iki	Pu'u 'Ō'ō	Etna 2001	Etna 2002–2003
Total duration (days)	35	+7890	23	65
Duration of cone growth (days)	35	1271	12	34
Widespread tephra volume (m^3)	1×10^7	N.D. [b]	5×10^6	4×10^6
Lava volume (m^3)	1.5×10^8	2×10^9	2.5×10^7	4×10^7
Immediate warning time (days)	1	1	6	2 h
First observed precursors (days)	90	26	4.5	<1
Cone area (ha)	40	610	28	32
Cone height (m)	50	255	62	150
Cone growth: average (m/day) [c]	1.4/3.7	0.20/5.4	5.2	4.1
Cone growth: maximum (m/day)	N.D. [b]	49	N.D. [b]	N.D. [b]
Maximum fountain height (m)	580	470	700	600
Maximum plume height (km)	N.D.	ND.	3–5	6
Maximum fissure length (km)	1	7.5	5	11

[a] Source references are: Kīlauea Iki 1959 (Macdonald, 1962; Richter et al., 1970; Eaton et al., 1987; Parfitt, 1998), Pu'u Ō'ō (Heliker et al., 2003; Heliker and Mattox, 2003), Etna 2001 (Behncke and Neri, 2003; Calvari and Pinkerton, 2004) and Etna 2002–2003 (Andronico et al., 2004).

[b] N.D. not determined.

[c] For Kīlauea Iki and Pu'u 'Ō'ō , the first number is an average including the duration of pauses between episodes and the second is an average for growth rate based only on time in eruption.

The most widespread hazard during such eruptions is the accumulation of tephra falls over distances of typically a few kilometers from source (Blong, 1984, 2003). The tephra fall deposit typically has two elements: a cone surrounding the vent and a more widespread blanket of ash and lapilli. There are few accounts of rates of tephra fall accumulation during such eruptions and how quickly key thresholds in tephra thickness will be achieved at given distances from source. In this paper, we take data from four recent historical eruptions (Table 1) and apply them to the Auckland volcanic field (Fig. 1). These eruptions were chosen from among the wider range of documented historical cone-forming eruptions for completeness of the record of tephra accumulation and particularly for rates of cone growth. They compare well with the Auckland prehistoric cones in terms of both eruption type (Hawaiian, Strombolian and effusive) and in terms of eruption volume (judged from cone dimensions).

2. Background

2.1. Auckland volcanic field

Auckland is New Zealand's largest urban centre, with some 1,173,000 residents, (2001 census data) and lies entirely within the Auckland volcanic field. The field, covering an area of 360 km^2, has some 49 individual eruptive centers of basaltic composition (Fig. 2), which have displayed a range of effusive, Strombolian, Hawaiian and phreatomagmatic eruptive styles (Searle, 1962; Rout et al., 1993). The eruptions have produced a large number of volcanic cones ranging in radius from 230 to 580 m (average 400 m) and area from 17 to 54 ha (average 54 ha) together with a lesser number of maars and tuff rings. Each cone formed during episodes of Strombolian and/or Hawaiian fire fountaining commonly accompanied by phreatomagmatic episodes. The largest and most recent eruption formed Rangitoto lava shield less than 800 years ago (Allen and Smith, 1994).

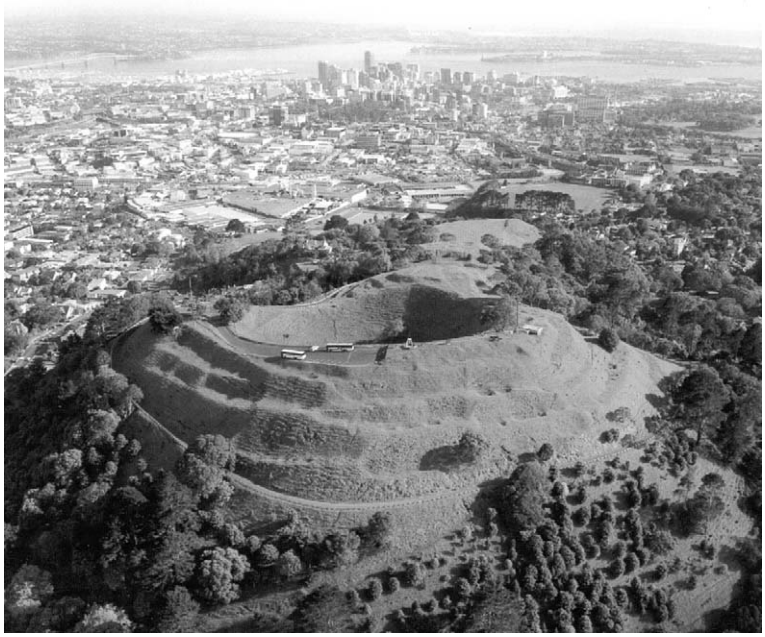

Fig. 1. Aerial view of Auckland city with Mt. Eden scoria cone in foreground. Central business district is visible in centre, middle distance. Photo: D.L. Homer.

2.2. Potential economic impact of future eruptions

Paton et al. (1994) present a quantitative assessment of risk from future eruptive activity at Auckland, based on five scenarios developed by Johnston et al. (1997). The evaluation included both direct (damage to buildings and properties) and indirect (loss of business, costs of evacuation, relocation) consequences of the eruption. A future eruption will result in considerable destruction of property due to the high population density and significantly higher costs associated with clean-up of tephra. Paton et al. (1994) estimate the latter to range between NZ$58M and NZ $243 (ca. US$38M and US$159M) for their five scenarios. Two newly published papers evaluate comparative risk in the Auckland region for several potential sources (Magill and Blong, 2005a,b); this study focuses only on future explosive eruptive activity from the Auckland volcanic field.

2.3. Scenarios

In the scenarios developed by Johnston et al. (1997), five source vents are chosen and a different scenario is developed for each. Hazards include lava effusion, phreatomagmatic, Hawaiian and Strombolian explosive activity, accompanied by lightning, acidic aerosols, and ground cracking and shaking. The cumulative impacts were then evaluated for each scenario. Three of the scenarios involve vent sites onshore (Fig. 3), where rapid cone growth and widespread lapilli-ash fall are likely.

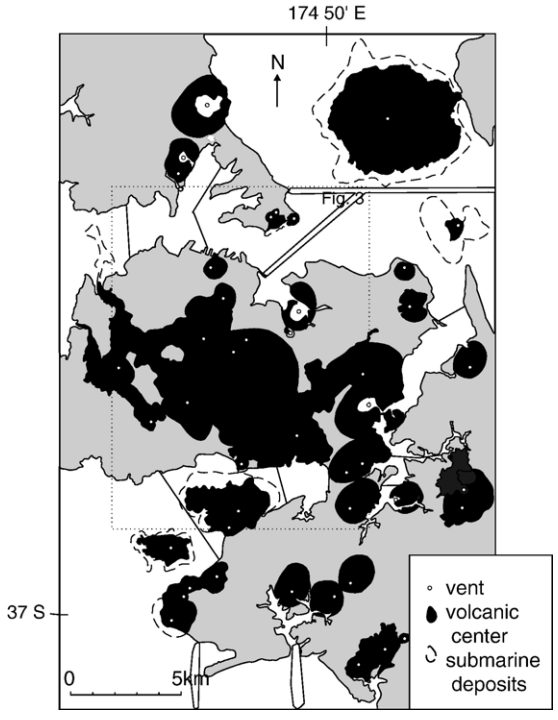

Fig. 2. Location map showing distribution of eruptive centers used in scenarios by Johnston et al. (1997) and Paton et al. (1994).

3. The historical case studies

The four eruptions summarized in Table 1 were selected because of the completeness of the records describing the activity and its impacts. Two are of mixed effusive (both ʻaʻā and pahoehoe) and Hawaiian character (Kīlauea Iki 1959, Puʻu ʻŌʻō 1983–1986), and two are characterized by Hawaiian and Strombolian explosive activity and accompanying ʻaʻā lava effusion (Etna 2001, 2002–03). In this study, we focus only on the explosive phases of activity in each eruption. This is an important qualifier as in three of the four eruptions the social and economic impacts of lava effusion were far more significant. Another very important caveat is that all four eruptions occurred in national parks well away from any urban areas; impacts accordingly were far less than for any future eruption in the Auckland field.

3.1. Kīlauea Iki 1959 eruption

An erupting fissure formed at 8:08 p.m. on November 14, 1959, 100 m above the floor of Kīlauea Iki crater, a prehistoric collapse pit (Richter et al., 1970). In less than 24 h, only one vent remained active. Scoria, spatter and pumice fell downwind of the vent building the first parts of a new scoria cone and a scoria-pumice blanket to the south (Fig. 4). Fountain-fed lava drained northward onto the floor of Kīlauea Iki crater forming a lava lake. Seven days later, the fountain collapsed in less than 40 s, ending Episode 1. The next 16 episodes were superficially similar to the first, but with subtle and interesting contrasts. In particular (Fig. 5), there was a wide range in duration of the episodes (2 h to 8 days) and in the lengths of intervening periods of repose (8 h to 4 days). Characteristics of the episodes are summarized by Macdonald (1962), Richter et al. (1970) and

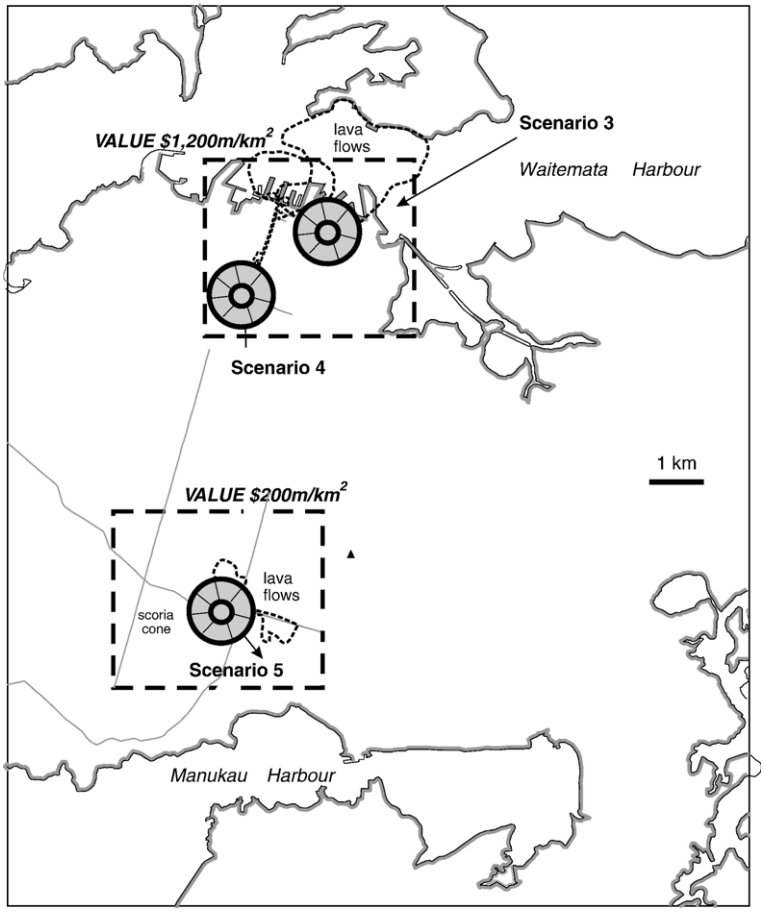

Fig. 3. Location map for on-land scenarios used by Johnston et al. (1997) and Paton et al. (1994). Cones are drawn around their proposed vents, with a radius of 600 m, following the logic given in the text. Dashed lines outline lava flows from their scenarios. Values quoted in NZ$ km^{-2} are estimates for the value of real estate in the downtown area (scenarios 3 and 4) and the suburbs affected by scenario 5, respectively.

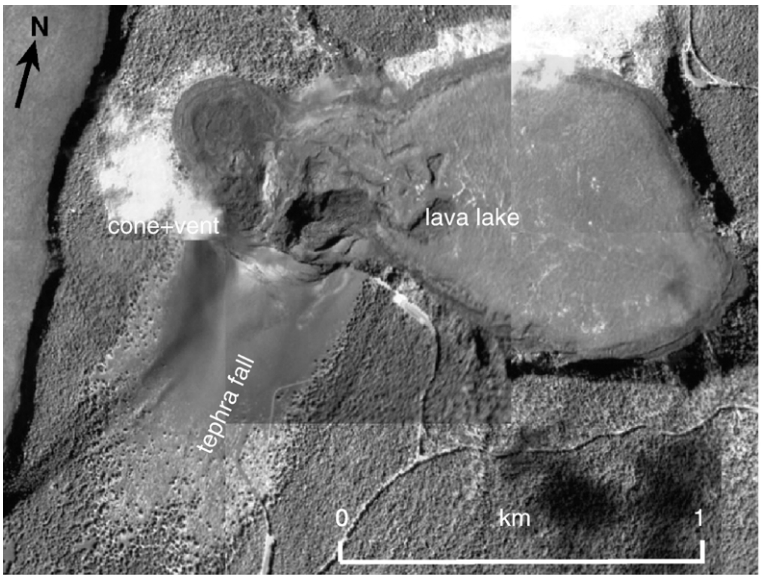

Fig. 4. False color satellite image of Kīlauea Iki area showing the proximal cone and vent, widespread tephra fall to the southwest and the lava lake ponded in the pre-existing collapse crater. Image courtesy of Peter Mouginis-Mark.

Eaton et al. (1987). The end of the eruption came relatively abruptly after two episodes of fountaining to 450–550 m height (Fig. 5).

3.2. Episodes 1 to 48 of the Kīlauea 1983–present eruption

The current eruption of Kīlauea volcano began on 3 January 1983. The first 3.5 years of this eruption built a 255-m high cone at Pu‘u ‘Ō‘ō on the volcano’s east rift zone (Heliker et al., 2003; Heliker and Mattox, 2003). Explosive activity was accompanied by effusion of 5×10^8 m^3 of lava (a total of 2 km^3 of lava have been erupted to August 2004). The 48 episodes until June 1986 were remarkably regular, ranging in duration from 5 h to 4 days, with repose periods of between 8 and 65 days (Heliker and Mattox, 2003). The rates of cone growth were measured with unique detail (Heliker et al., 2003), but the more widespread lapilli and ash fell in remote areas and there is little information about accumulation rates or even thickness.

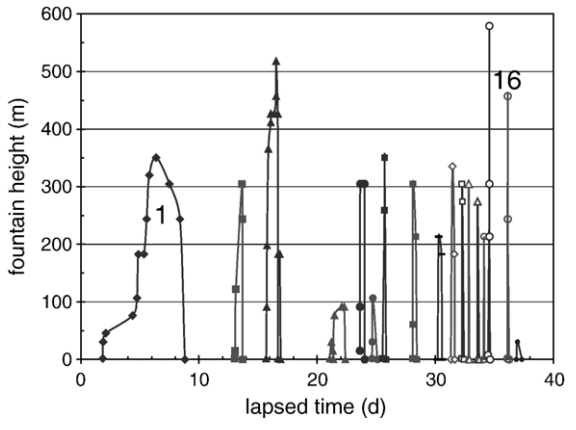

Fig. 5. Plot of fountain height with time for the Kīlauea Iki 1959 eruption using data from Richter et al. (1970). Key episodes used to quantify accumulation rates of tephra are numbered.

3.3. Etna 2001: Laghetto cone

The July–August 2001 eruption of Etna volcano took place along a 5-km long fissure with explosive activity focused on two clusters of vents at 2100 m and 2550 m elevation on the southern flank of the volcano (INGV Staff, 2001; Behncke and Neri, 2003; Calvari and Pinkerton, 2004). A 62-m high cone formed at the 2550-m vent, principally between 25 and 31 July (Calvari and Pinkerton, 2004). Deposition of a widespread ash and scoria blanket from these vents *preceded* cone growth—a phase of violent phreatomagmatic explosions between 19 and 24 July deposited ash downwind as far as northern Africa and closing two major airports. Vigorous cone growth followed during a period of fire-fountaining with very little widespread tephra fall. In August, activity reverted to weaker phreatomagmatic explosions lasting until 9 August.

3.4. Etna 2002–2003

The 3-month long eruption of Etna between October 2002 and January 2003 took place from fissures extending approximately 11 km over the northern and southern flanks of the volcano. Ground cracking preceded the eruption by 7 months; intense seismicity only commenced on the first day of the eruption but caused intense damage in two villages. Early Strombolian, phreatomagmatic and effusive activity was replaced by a period of intense fountaining, cone growth and deposition of widespread ash until 12 November. Subsequent explosive activity concentrated at the 2750-m vent was characterized by alternation Hawaiian and Strombolian eruption. From 10 December, there was a gradual decrease in eruptive intensity with abrupt shifts between fountaining and Strombolian explosions on a scale of hours. Two major cones formed on the southern rift zone, at 2750 to 2800 m elevation, and lava flows traveled 6.2 km (NE rift) and 3.6 km (southern rift) from source (Andronico et al., 2004).

3.5. Summary and comparisons

The four eruptions offer us complimentary data sets to approach the issues of hazard and risk at Auckland. For example, the record of rate of cone growth is excellent for Pu‘u ‘Ō‘ō but poor for Kīlauea Iki; yet the widespread tephra blanket is poorly preserved at Pu’u Ō’ō and well exposed at Kīlauea Iki.

All four eruptions had fissure sources but with mass discharge strongly focused on only one or two locations on the fissures. While remaining on the growing cones, the exact vent positions shifted in seemingly random fashion in each case. Intervals of cone growth in the four eruptions lasted between 12 days and 3.5 years, but average rates of growth during eruption were remarkably consistent at 4–6 m/day. Data for the one eruption where growth rates are extremely well constrained, Pu’u Ō’ō, suggest that peak instantaneous rates are an order of magnitude higher, as high as 1–2 m/h. Cone growth was essentially continuous for the Etna eruptions and episodic for the two Kīlauea eruptions. Formation of a widespread tephra blanket *preceded* cone growth in the 2001 Etna eruption but occurred during cone construction in the other three eruptions. In every case, the onset of definitive precursors linked to the eruption, and permitting specific eruption forecasts, was very short—typically days.

Table 2
Summary of impacts from the modern case studies[a]

Eruption: tephra	Kīlauea Iki	Pu‘u ‘Ō‘ō	Etna 2001	Etna 2002–2003
Building collapse	Yes	N/A	No	Yes
Building damage	Yes	N/A	Yes	Yes
Road closures	Yes	No	Yes	Yes
Airport closures	No	No	Several days	2 weeks
Water/storm water systems	N/A	N/A	Yes	Yes
Related impacts				
Buildings destroyed by lava flow	No	No	Yes	Yes
Buildings destroyed by cracking	No	No	No	Yes
Forest fires	Yes	Yes	Yes	Yes

[a] Source references are as for Table 1.

3.6. Impacts

All four eruptions included both explosive and effusive products but we focus here on the impacts of tephra accumulation. The cones (or cone clusters) grew in areas of national parks remote from buildings but the Kīlauea Iki 1959 cone grew across and forced the permanent diversion of Crater Rim Drive, the major access road inside the national park. Isolated park buildings, less than 1 km downwind from the vent, were destroyed by roof collapse due to tephra fall in the 1959 eruption and in the Etna 2002–2003 eruption. Eruption plumes and distal tephra accumulation forced closure of two major airports in Sicily and Calabria in both 2001 and 2002. A major tephra cleanup operation was necessary during both Etna eruptions (Behncke and Neri, 2003; Andronico et al., 2004). The impacts of lava flows were considerable in all but the Kīlauea Iki 1959 eruption (where lava ponded in an adjacent pit-crater), destroying roads, buildings and, at Etna, ski-field facilities (Table 2).

4. Hazard evaluation

We take a complimentary approach here to that of Johnston et al. (1997) in considering how quickly key thresholds of tephra thickness might be achieved in Auckland, based on data from four very recent basaltic explosive eruptions. We have divided this evaluation into two regions of tephra accumulation, the cone and the widespread tephra blanket. For both, we consider the time required to achieve critical thresholds of tephra thickness that equate to onset of types of impact.

4.1. Critical thresholds of tephra fall

We list critical damage thresholds for tephra fall cited by various authors in Table 3. Where values were quoted in kg m^{-2}, we have converted this to an equivalent thickness of basaltic tephra using a density value of 1320 kg m^{-3} determined for the Etna 2001 deposit (P. Del Carlo, unpublished data, 2005). From these values, we have selected the thresholds listed in Table 4 for use in this paper.

5. Cone growth and accompanying hazards

Hawaiian/Strombolian cones represent extreme environments of tephra accumulation with respect to all styles and intensity of explosive volcanism. The most rapid growth of cones often occurs during intervals of weaker explosions when a large proportion of the mass of ejecta falls very close to the cone rim, rather than at the peak of eruptive intensity.

Table 3
Some cited values for damage thresholds from tephra fall

Damage threshold	Thickness	Mass/area	Equiv. thickness	Source
	cm	kg m^{-2}	cm	
Airport closures		1	0.1	Del Carlo, unpub. data, Etna 2002
Damage to vegetation	1			Johnston et al. (1997)
Damage to vegetation		12	0.9	Bonadonna et al. (2002b)
Agricultural damage		1	.1	Del Carlo, unpub. data, Etna 2002
Partial loss of vegetation 1		180	13.8	Blong (1984)
Partial loss of vegetation 2		600	46.2	Blong (1984)
Near total vegetation kill		1800	138.5	Blong (1984)
Total vegetation kill		2500	192.3	Blong (1984)
Some roof collapse	30			Johnston et al. (1997)
Some roof collapse		120	9.2	Bonadonna et al. (2002b)
Total roof collapse	100			Johnston et al. (1997)
Total roof collapse		250	19.2	Bonadonna et al. (2002b)
Building damage V1		200	15.4	Blong (2003)
Building damage V3		305	23.5	Blong (2003)
Building damage V5		710	54.6	Blong (2003)

For values cited as mass/area conversions have been made assuming an in situ bulk density of 1300 km m^{-3}.

Table 4
Damage thresholds adopted in this paper

Damage threshold	Thickness (cm)
Closure of airports	0.1
Road closures, damage to vegetation	1
Minor roof damage (gutters, etc.)	15
Onset of roof collapse	25
Total roof failure	50

5.1. Rates of cone growth

The average rates quoted in Table 1 suggest that all the critical thresholds of tephra fall will be exceeded in the first day of explosive eruption, probably in the first 1–3 h. This means that there is little practical action that can be taken to mitigate this cone-forming tephra accumulation—the cone effectively defines a "red zone" of total destruction of structures and facilities. Areas incorporated in the four modern tephra cones ranged from 28 to 610 ha, equivalent to radii of 300 m to 1.4 km (Table 1). For comparison, the range among the 23 best exposed pre-historical Auckland cones (Fig. 1) is 17–100 ha (radii of 230 to 550 m). The initial zone affected by cone growth will be narrower—the cone grows radially as well as vertically but cones are steep and highly unstable and the cascading and tumbling of incandescent hot ejecta down the cone walls poses a threat to people and facilities beyond the margins of the cone. It therefore seems prudent to assume that the radius of the hazard zone for a future Auckland eruption could be of the order of 600 m. The scenarios within Johnston et al. (1997) used cones of radii 300 to 500 m.

Using data for building values in Auckland drawn from the Valuation New Zealand property database from 2002, we can estimate the financial impact of cone development for each of scenarios 3, 4 and 5, based on calculated average values shown in Fig. 3. For an eruption affecting the central business district, the impact will be very high (scenarios 3 and 4, Johnston et al., 1997). The cost for either scenario 3 or 4, both centered in the central business district, is likely to be at least NZ$1.4B (ca. US$900M). For a variety of reasons including inflation, this estimate is like to be a minimum. The impact is less for the vent for scenario 5, where cone growth is principally at the expense of

Table 5
Average accumulation rates of distal tephra inferred for 27–30 October 2002 during the Etna 2002–2003 eruption, mass/area data from Andronico et al. (2004)

Location	Rifugio Sapienza	Nicolosi	Catania
Distance (km)	4	16	28
Mass/area (kg m^{-2})	38.8	9.7	2.1
Equiv. thickness (mm)	30	7.5	1.5
Ave. accumulation rate (mm/h)	0.3	0.08	0.02

residential property, equating to damage of approximately NZ$200M (ca. US$130M).

5.2. Fissure development and ground cracking

A cautionary note is that all four recent case studies cited here involved multiple vents along fissures. Many such vents did not construct significant cones but associated hazards posed severe risks, e.g., from lava flows but also ground shaking and fracturing, as seen in both Etna eruptions. This suggests that the zone of highest risk is probably best defined as a narrow ellipse enclosing the principal vent site but extending for several kilometers in both directions.

6. Tephra blanket

The accumulation of widespread tephra blankets at Auckland is likely to be at rates that permit interventions by civil authorities to minimize damage. Measured rates for tephra fall from any historical eruptions are practically lacking. Following new field work at Kīlauea Iki, we are able to estimate accumulation rates for three of the most significant of the 17 eruption episodes and use these data to put some time constraints on emergency response times likely in a future Auckland eruption. Andronico et al. (2004) quote thicknesses of tephra accumulated between 27 and 30 October during the 2002 Etna eruption, which can be converted in approximate average accumulation rates (Table 5). These values suggest that, at distances of 5 to 30 km downwind from source, it would take several days of eruption to reach key thresholds of tephra fall for damage to vegetation or disruption of ground transport and major damage to building structures would be unlikely. However, for a future Auckland eruption, it is highly likely that buildings and key infrastructure will also lie between 1 and 5 km from vent. No direct data are available for accumulation rates at such distances. Instead, we use new field work to infer probable average rates of tephra accumulation for three episodes of the 1959 eruption.

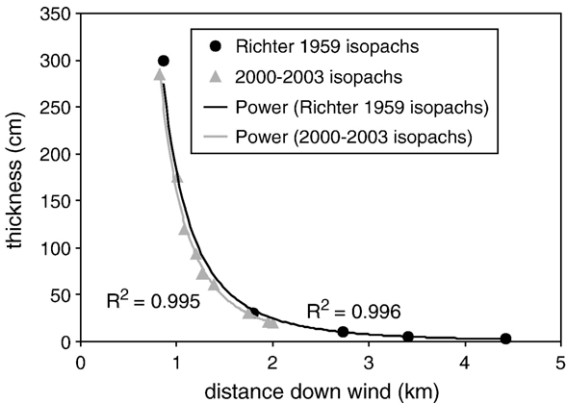

Fig. 6. Plot of thickness variation with distance downwind from the 1959 Kīlauea Iki vent. Data from Richter et al. (1970) and the authors' unpublished data collected between 2000 and 2004. Both datasets are fit equally well by power law thinning relationships.

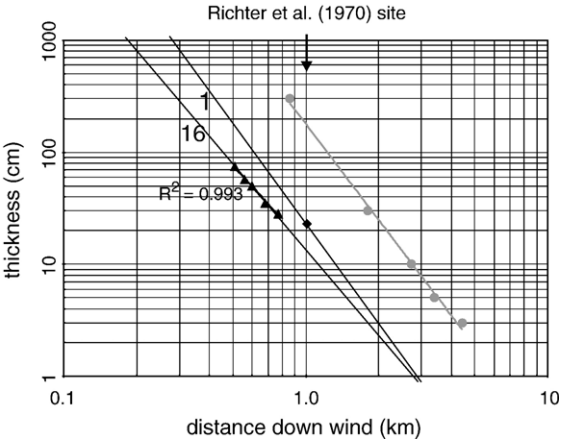

Fig. 7. Log–log plot of thickness versus downwind distance used to calculate accumulation rates for the episodes 1 and 16 of the Kīlauea Iki 1959 eruption. Accumulation rates for episode 16 are based on the thinning relationship observed in tephra pits along the dispersal axis. For episode 1, we calculate accumulation rates by fitting the power law relationship observed for the whole deposit to the thickness value measured by Richter et al. (1970) at 1.01 km from source.

6.1. Rates of tephra accumulation

The thickness distribution of the entire Kīlauea Iki 1959 distal tephra was mapped by Richter et al. (1970) and is shown as a downwind traverse in Fig. 6, along with new thickness data that we acquired between 2000 and 2004. The new data predictably follows the 1970 trend closely with a slight reduction in thickness at all sites due to compaction. The new data augments the 1970 data in a critical range of 1 to 2 km from source. Both sets of data are fit well by power law relationships

Table 6
Inferred times to reach key thresholds for tephra thickness at distances of 0.5, 1.0 and 5.0 km from vent based on data inferred for episodes 1 and 16 of the 1959 Kīlauea Iki eruption

Thickness (cm)	Threshold	Episode 1			Episode 16		
		0.5 km	1 km	5 km	0.5 km	1 km	5 km
		Time (h)	Time (h)	Time (h)	Time (h)	Time (h)	Time (h)
0.1	Airport closure	0.1	0.7	73	.004	.03	1.0
1	Road closure, plant damage	1.0	7	*726*	.04	.25	*10*
15	Minor roof damage	16	109	*10892*	0.62	3.8	*145*
25	Onset roof collapse	26	182	*28152*	1.0	*6*	*242*
59	Total roof failure	52	*363*	*36304*	2.1	*13*	*484*

Values in italics indicate durations longer than those of the episodes in question.

(Figs. 6 and 7). The data for whole-deposit thickness are of limited value in estimating accumulation rates because of the lengthy breaks between episodes and the contrasting fountain heights and therefore intensities (Fig. 5) both during and between episodes. If we could constrain thinning rates for individual episodes, however, then we could use the known durations of those episodes to arrive at accumulation rates. We have attempted this in two different ways for episodes 1 and 16. Richter et al. (1970) measured, at one site, 1.01 km downwind from vent, the thickness of the deposits from episode 1 as 0.23 m (Fig. 7). Episode 1 was the longest episode (Fig. 5), longer in duration than the *sum* of all the remaining 16 episodes combined (167 h versus 157 h, respectively) and was of intermediate intensity. As such, it contributes significantly to the slope of the total deposit curve in Fig. 7. Also at this site, and neighboring sites between 0.5 and 0.8 km of the vent, we have identified and measured the thickness of the deposit from episode 16 (Fig. 7), the last high fountaining episode during the eruption (Fig. 4). At sites between 0.5 and 0.8 km downwind from vent, the total thickness of the deposit precludes us from measuring the episode 1 deposits. The new data for the episode 16 deposits are also fit well by a power law (Fig. 7) with predictably slightly slower thinning rate than for the whole deposit (this was expected as episode 16 was one of the highest fountaining events). We have used this curve to constrain thinning rates for episode 16. We have fit a second curve parallel to that of the whole deposit through the single thickness value for episode 1, reflecting its very average fountain height and intensity. Using these data, we have then calculated average accumulation rates for each episode at distances of 0.5, 1 and 5 km downwind from source (Table 6).

The data show predictably that the lapsed times, needed to achieve a critical tephra thickness at any distance from vent, vary considerably with eruptive intensity, e.g., between 2 h and 2 days to achieve widespread roof collapse 500 m from source. However, some generalizations can be made:

(1) *5 km from vent:* Most tephra thresholds are unlikely to be achieved in any one eruption episode. With even the highest accumulations rates, it would take 10 h to accumulate 1 cm of ash on roadways. Hazard is likely to be restricted to nuisance value only.
(2) *1 km from vent:* Total roof failure would require high eruption rates to be sustained for more than 12 h. (Major roof collapse is unlikely with lower accumulation rates.) During this period, there is opportunity to remove people and key resources from the hazard zone and to contemplate ash removal from roof structures. However, actions will be hindered by the effects of tephra fall on ground transportation—accumulation of 1 cm of ash on roadways is likely to occur within 15–30 min. A key question for emergency managers is whether this is enough lead-time to order the removal of non-essential vehicles from the hazard zone.
(3) *0.5 km from vent:* Severe damage to buildings and infrastructure is likely to occur at this distance, close to the margin of the growing cone. In all scenarios, road closures are likely in less than an hour and structural damage to buildings will begin between 1 h and 1 day after the onset of eruption.

6.2. Probabilistic approach to wind direction

Wind directions play a critical role in influencing the pattern of distal dispersal of tephra. The modern eruptions used here as case studies took place under different sets of wind conditions. The two Kīlauea eruptions took place predominately under stable trade wind conditions so that ejecta accumulated preferentially

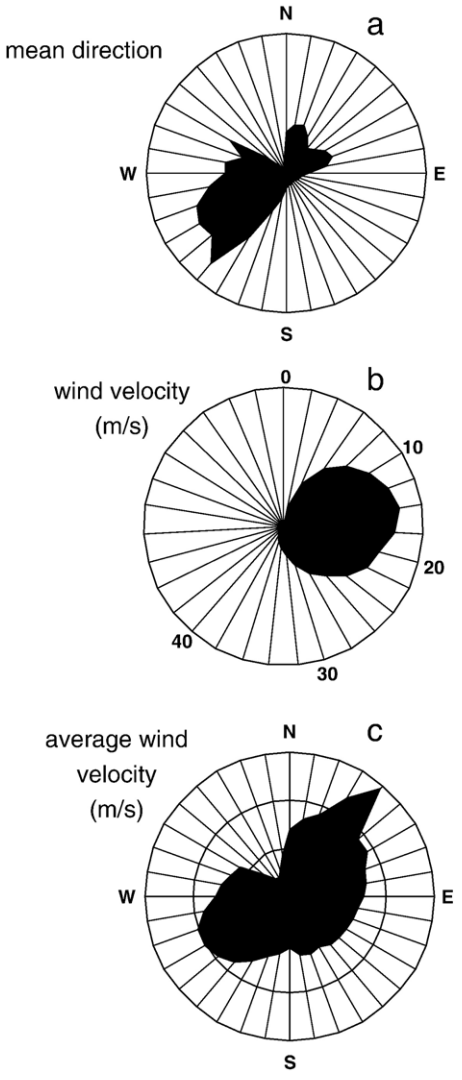

Fig. 8. Wind direction and wind velocity measured at a meteorological station located at 300 m a.s.l. on the Auckland Sky Tower (hourly data between 5/1/2001 and 6/30/2004).

to the SW of Kīlauea Iki and Pu'u Ō'ō. During the 2001 and 2002–2003 eruptions of Etna, fluctuating wind velocity carried the tephra fall at various times to the N, NE, E, SE and S (Andronico et al., 2004). The Auckland climate is also characterized by fluctuating wind velocities (Fig. 8). In addition, tephra dispersal from cone-forming eruptions would mainly be affected by low-level wind (i.e., <1 km a.s.l.), which is typically more variable than high-level wind. We have analyzed wind data for direction and velocity directly measured on a meteorological station located on the Auckland Sky Tower at 300 m a.s.l., and within 2 km of the vent sites for scenarios 3 and 4 of Johnston et al. (1997). Measurements were taken every hour between 1 May 2001 and 30 June 2004 with a total of 25,755 data points. Fig. 8 shows that the principal wind directions lie between 220° and 300° (55% of the data) and 0° and 80° (27% of the data). All directions are expressed in degrees from N. The average wind velocity is 16 m s^{-1} with a standard deviation of 8 m s^{-1} and the most common wind velocity is 14 m s^{-1} (Fig. 8b). A detailed analysis of wind velocity and direction also shows that winds blowing from NE are characterized by the highest mean wind velocity (i.e., 29 m s^{-1}; Fig. 8c).

The extended duration of cone-forming eruptions means that, to assess the influence of eruption duration on

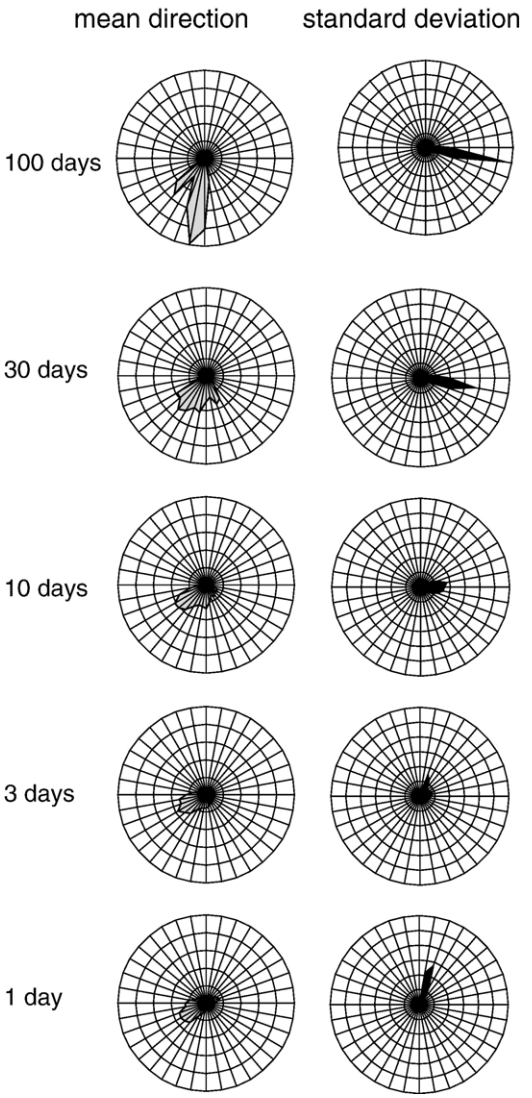

Fig. 9. Mean wind directions and standard deviations calculated for 10,000 Monte Carlo simulations of 1-, 3-, 10-, 30- and 100-day duration.

tephra dispersal, we have run Monte Carlo simulations and stochastically sampled sequential wind data for eruption scenarios of durations 1, 3, 10, 30 and 100 days. In each case, we have performed 10,000 runs based on random selections of the start point for each simulation (Fig. 9) from among the 2001–2004 wind data in Fig. 8. As expected, the mean wind direction varies the most for the short-duration scenarios, whereas the long-duration scenarios are characterized by the largest standard deviation (Fig. 9). As an example, directions for a 100-day scenario vary between 10° and 360° with mean directions between 160° and 240° and standard deviations between 70° and 120° (Figs. 9 and 10). In contrast, mean directions for a 1-day scenario vary between 20° and 330° with 20% of values between 20° and 100° and 65% of values between 180° and 300°. Corresponding standard deviations vary between 10° and 180° with 60% of the values between 10° and 30° (Figs. 9 and 10). The mean directions for the 1-day scenario resemble the whole dataset of Fig. 8, being characterized by two main populations to the WSW and the ENE, respectively.

We need to bear in mind that the mean wind directions do not necessarily indicate realistic values unless they are analyzed together with the corresponding standard deviations. This is true above all when the variation range is large like in the case of the 100-day scenario, i.e., 10–360°. Mean wind directions for the 1-day scenario in Fig. 9 show similar characteristics to the general plot in Fig. 8 because they result from an average of fewer values (i.e., 24 hourly wind data for each run) and the corresponding standard deviations are relatively small (i.e., mostly 10–30°). However, the mean directions for the 100-day scenario result from the average of more values (i.e., 2400 hourly wind data for each run) and therefore they plot between the two main populations in Figs. 8 and 9. As a result, the corresponding standard deviations for the 100-day duration are large, i.e., 70–120°.

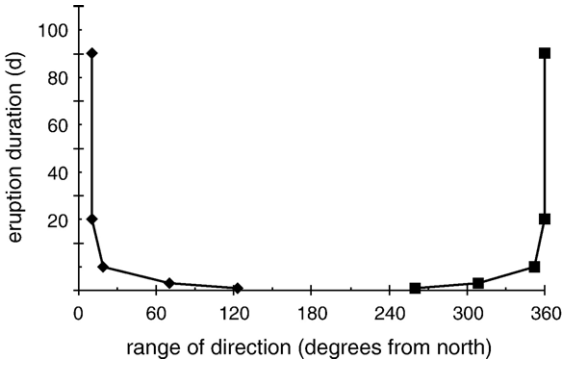

Fig. 10. Variation of average minimum and maximum wind direction recorded during the simulations in Fig. 9, i.e. for duration of 1, 3, 10, 30 and 100 days.

In conclusion, wind directions during eruptions of long duration are expected to vary significantly and thus net accumulation rates of tephra at any point will be reduced, whereas tephra dispersal during short-lived eruptions is more likely to be narrowly dispersed to the ENE or the WSW, in line with the seasonal variations of wind directions observed at Auckland.

7. Conclusions

The Auckland region is both a major metropolitan area and a concentration of young basaltic volcanoes. The high density of buildings and lifelines, in particular, poses special problems, which are exacerbated by the high probability that future eruptions will be of prolonged duration. Any explosive eruption from a vent on-land is likely to involve cone-forming Strombolian and/or Hawaiian phases. Our analysis suggests that little can be done to mitigate the deposition of tephra close to the vent site, i.e., in forming the cone(s); accumulation rates will be typically several meters per day. The only solution within the area of the rapidly growing cone (a region of c.600 m radius from vent) is to quickly establish an exclusion zone to protect human life. However, accumulation rates of tephra *beyond* and downwind of the cone will be much lower, e.g., probably between 4 and 110 h for the onset of minor damage to buildings. Our analysis of 2001–2004 wind data suggests that during any prolonged eruption tephra fall will be dispersed in most quadrants as the eruption progresses. Emergency managers therefore face the difficult decision of whether it is preferable to allow residents and workers to remain or re-visit facilities in order to clear tephra fall and minimize damage or to evacuate a larger “red zone” which we suggest would probably be of approximately 5 km radius.

This study does not touch on some other important aspects of hazard and risk at Auckland—the threat from lava flows, damage from ground shaking and formation of fissures and cracking, or the possibility of violent phreatomagmatic explosions driven either by ground water or seawater, which should be the focus of future work.

Acknowledgements

This manuscript benefited greatly from constructive comments by Russell Blong and Marta Calvache and particularly editorial review by Lionel Wilson. The research was supported by NSF EAR–0409303

(Houghton), NSF EAR–0456518 (Bonadonna) and grants from the New Zealand Foundation for Research Science and Technology (Cole, Houghton).

References

Acocella, V., Neri, A., 2003. What makes flank eruptions? The 2001 Etna eruption and its possible triggering mechanisms. Bulletin of Volcanology 65, 517–529.

Allen, S.R., Smith, I.E.M., 1994. Eruption styles and volcanic hazard in the Auckland Volcanic Field, New Zealand. Geoscience Reports of Shizuoka University 20, 5–14.

Andronico, D., Branca, S., Calvari, S., Burton, M., Caltabiano, T., Corsaro, R.-A., Del Carlo, P., Garfì, G., Lodato, L., Miraglia, L., Murè, F., Neri, M., Pecora, E., Pompilio, M., Salerno, G., Spampinato, L., 2004. A multi-disciplinary study of the 2002–03 Etna eruption: insights into a complex plumbing system. Bulletin of Volcanology (ISSN: 0258-8900), 55–77 (Published on-line July 2004).

Barberi, F., Murgia, C., Brondi, F., Carapezza, M.L., Cavarra, L., 2003. Earthen barriers to control lava flows in the 2001 eruption of Mt. Etna. Journal of Volcanology and Geothermal Research 123, 231–243.

Behncke, B., Neri, M., 2003. The July–August 2001 eruption of Mt. Etna (Sicily). Bulletin of Volcanology 65, 461–476.

Blong, R.J., 1984. Volcanic hazards. A Sourcebook on the Effects of Eruptions. Academic Press, Sydney. 424 pp.

Blong, R., 2003. Building damage in Rabaul, Papua New Guinea, 1994. Bulletin of Volcanology 65 (1), 43–54.

Bonadonna, C., Macedonio, G., Sparks, R.S.J., 2002a. Numerical modelling of tephra fallout associated with dome collapses and Vulcanian explosions: application to hazard assessment on Montserrat. In: Druitt, T.H., Kokelaar, B.P. (Eds.), The Eruption of Soufrière Hills Volcano, Montserrat, from 1995 to 1999. Geological Society, London, Memoir.

Bonadonna, C., Mayberry, G.C., Calder, E.S., Sparks, R.S.J., Choux, C., Jackson, P., Lejeune, A.M., Loughlin, S.C., Norton, G.E., Rose, W.I., Ryan, G., Young, S.R., 2002b. Tephra fallout in the eruption of Soufrière Hills volcano, Montserrat. In: Druitt, T.H., Kokelaar, B.P. (Eds.), The Eruption of Soufrière Hills Volcano, Montserrat, from 1995 to 1999. Geological Society, London, Memoir.

Calvari, S., Pinkerton, H., 2004. Birth, growth and morphologic evolution of the 'Laghetto' cinder cone during the 2001 Etna eruption. Journal of Volcanology and Geothermal Research 132, 225–239.

Eaton, J.P., Richter, D.H., Krivoy, H.L., 1987. Cycling of magma between the summit reservoir and Kilauea Iki Lava Lake during the 1959 eruption of Kilauea volcano. U.S. Geological Survey Professional Paper 1350, 1307–1335.

Heliker, C.C., Mattox, T.N., 2003. The first two decades of the Pu'u 'O'o-Kupaianaha eruption: chronology and selected bibliography. U.S Geological Survey Professional Paper 1676, 1–28.

Heliker, C.C., Mangan, M.T., Mattox, T.N., Kauahikaua, J.P., Helz, R.T., 1998. The character of long-term eruptions—inferences from episodes 50–53 of the Puu Oo-Kupaianaha eruption of Kilauea volcano. Bulletin of Volcanology 59, 381–393.

Heliker, C.C., Kauahikaua, J., Sherrod, D.R., Lisowski, M., Cervelli, P.F., 2003. The rise and fall of Pu'u 'O'o Cone, 1983–2002. U.S. Geological Survey Professional Paper 1676, 29–51.

Hildreth, E.W., 1987. New perspectives on the eruption of 1912 in the Valley of Ten Thousand Smokes, Katmai National Park, Alaska. Bulletin of Volcanology 49, 680–693.

INGV Staff, 2001. Multidisciplinary insights into the 2001 Etna flank eruption. EOS 82, 653–656.

Johnston, D.M., Nairn, I.A., Thordarson, T., Daly, M., 1997. Volcanic impact assessment for the Auckland volcanic field. Auckland Regional Council Technical Publication 79 (208 pages).

Macdonald, G.A., 1962. The 1959 and 1960 eruptions of Kilauea volcano, Hawaii, and the construction of walls to restrict the spread of the lava flows. Bulletin Volcanologique 24, 249–294.

Magill, C., Blong, R., 2005a. Volcanic risk ranking for Auckland, New Zealand: I. Methodology and hazard investigation. Bulletin of Volcanology 63, 331–339.

Magill, C., Blong, R., 2005b. Volcanic risk ranking for Auckland, New Zealand: II. Hazard consequences and risk calculation. Bulletin of Volcanology 63, 340–349.

Parfitt, E.A., 1998. A study of clast size distribution, ash deposition and fragmentation in a Hawaiian-style volcanic eruption. Journal of Volcanology and Geothermal Research 84, 197–208.

Parfitt, E.A., Wilson, L., 1994. The 1983–86 Pu'u O'o eruption of Kilauea volcano, Hawaii—a study of dike geometry and eruption mechanisms for a long-lived eruption. Journal of Volcanology and Geothermal Research 59, 179–205.

Paton, D., Johnston, D., Gough, J., Dowrick, D., Manville, V., Daly, M., Batistich, T., Baddon, L., 1994. Auckland volcanic risk project: stage 2. Auckland Regional Council Technical Publication 126 (99 pages).

Richter, D.H., Eaton, J.P., 1960. The 1959–60 eruption of Kilauea volcano. New Scientist 7, 994–997.

Richter, D.H., Eaton, J.P., Murata, K.J., Ault, W.U., Krivoy, H.L., 1970. Chronological narrative of the 1959–60 eruption of Kilauea volcano, Hawaii. U.S Geological Survey Professional Paper 537-E (73 pp.).

Rout, D.J., Cassidy, J., Locke, C.A., Smith, I.E.M., 1993. Geophysical evidence for temporal and structural relationships within the monogenetic basalt volcanoes of the Auckland volcanic field, northern New Zealand. Journal of Volcanology and Geothermal Research 57, 71–83.

Searle, E.J., 1962. The volcanoes of Auckland city. New Zealand Journal of Geology and Geophysics 5, 193–227.

Wolfe, E.W., Hoblitt, R.P., 1996. Overview of the eruptions. In: Newhall, C.G.P., R.S. (Eds.), Fire and Mud: Eruptions and Lahars of Mount Pinatubo, Philippines. Washington Press, Seattle.